Benchmarking the 2D Lattice Boltzmann BGK Model

Simon T. Engler

Universiteit van Amsterdam, Faculty of Naturrkunde
Amsterdam Center for Computational Science, Amsterdam, The Netherlands
e-mail: sengler@science.uva.nl

Abstract

A 2D Lattice Boltzmann BGK (LBGK) model on a D2Q9 lattice was constructed and tested for accuracy in different physical situations. An introduction to the LBGK method is given followed by a detailed outline of the computer model construction. Due to the fact that LBGK models are restricted to low Reynolds numbers only laminar fluid flow is examined here. The model was tested for accuracy by comparing model output to the analytical solution of flow lines past a right circular cylinder. Next, plane Poiseuille flow through a 2D channel is compared to the analytical fluid flow and pressure solutions.

1. Introduction

There are many different forms of Lattice Boltzmann Models (LBMs) available to the computational scientist today. Like in any simulation situation the choice unto which type of model that can be used is determined by the necessity of model accuracy over computational speed. In the case of a full-blown Lattice Boltzmann model, one is capable of recovering the full Navier-Stokes equations to good accuracy. However, this accuracy comes at relatively high programming complexity and computational expense. One of the major components of the computational expense in the LBMs is due to the evaluation of the particle collision and equilibrium distribution operators that need to be solved.

The Lattice Boltzmann BGK model (LBGK) was developed using an approximation to the equilibrium distribution to cut down the cost of computation. Like any approximation within a mathematical procedure, there will be a loss in the accuracy of the solution. In order for the computational scientist to apply the LBGK effectively it is necessary for the scientist to understand the exact limitations of the model under a variety of situations.

Benchmarking a model under several well-known and understood analytical solutions to physical situations is the best way to find and understand the accuracy and limitations of any computational model. The LBGK model was constructed and then benchmarked through two different physical situations.

Laminar fluid flow past a right circular cylinder benchmarks the model's capability to simulate flow past an obstacle. This is done through the comparison of simulated flow lines to analytical flow lines, which are examined in this article.

Laminar Poiseuille flow through a 2D channel allows one to compare the fluid flow profile through the channel to the analytical solution. This shows the models capability to handle free fluid flow (non-obstructed). Flow through a channel also allows one to compare pressure solutions to the analytical solutions.

The construction of a LBGK model was carried out and subjected to the two benchmark situations described above. In this article, the theory and construction of this model are outlined in detail. Simulations were conducted under the

benchmark situations and examined. The results obtained should allow one to assess the suitability of the model for implementation into a simulation.

2. The Lattice Boltzmann BGK Model

The Lattice Boltzmann equation provides us with a way to simulate hydro dynamical flow as an alternative to using finite-element methods in computational fluid dynamic simulations. The Boltzmann model is constructed on a lattice space that contains fluid particles. Each of these particles is given a discrete set of velocities for travelling from one node on the grid to another. This represents particle advection. The particles are redistributed on each node according to a set of rules that recover the collision process. [7]

This model uses a D2Q9 lattice with nine discrete velocities that were originally outlined by Koelmann. These rules signify the advection step in the model of a particle from one node to

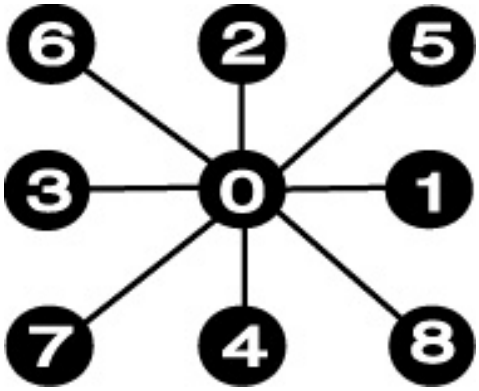

Figure 1: Node ordering on the DQ29 lattice

another over a specified velocity c. Table 1 shows the velocity distribution rules from node point zero to the neighbouring node points. Figure 1 displays the node ordering of the rules. By comparing Table 1 to Figure 1, one can see how the particle velocities are redistributed in the advection process.

The time evolution of the model is based upon particle distribution and collisions of the model. Time evolution is carried out during the propagation of the particles along the lattice points according to the rules described above.

Koelmann (1991) Lattice Velocities:
C{0} = (0,0)
C{1,3}=(±c,0)
C{2,4}=(0,±c)
C{5,6,7,8}=(±c,±c)

Table 1: Different lattice velocities associated to relative position on grid. Compare with Figure 1.

The collision process is mimicked by a distribution function rather than solving for collisions of every particle. Lattice-Boltzmann models are normally constructed using Fermi-Dirac or Maxwellian distributions as the collision process. [4] However, solving these distribution functions is complicated and computationally expensive. The single relaxation time BGK operator approach allows us to solve this equilibrium distribution such that the microscopic equations are satisfied and the Navier-Stokes equations are recovered. [4-5-6].

To formulated these ideas into a mathematical model the equilibrium distribution of the particles on the lattice shall be denoted as

$$\overline{F_i}(x,t) \quad (1)$$

The time evolution of the lattice BGK method is solved through [4,7,8]

$$F_i(x+c_i\Delta t, t+\Delta t) - F_i(x,t) = \Omega_i(x,t) \quad (2)$$

Here, $\Omega_i(x,t)$ is the single relaxation time BGK operator and is solved by [4,7,8]

$$\Omega_i(x,t) = -\frac{1}{t}\left[F_i(x,t) - \overline{F_i}(x,t)\right] \quad (3)$$

Here, $F_i(x,t)$ is the current distribution of particles on a lattice node. The symbol t is

the time relaxation parameter. $\overline{F}_i(x,t)$ is the equilibrium function. We shall denote the equilibrium distribution as:

$$\overline{F}_i(x,t) = E_i(r,u) \quad (4)$$

The equilibrium distribution is solved by considering hydrodynamic field density r, and discrete velocity m. [8] These moments are calculated through summing density and velocity over the lattice [8].

$$r(x,t) = \sum_{i=0}^{N} F_i(x,t) \quad m(x,t) = \sum_{i=0}^{N} c_i(x,t) \quad (5)$$

Finally, taking a Taylor expansion of the Fermi-Dirac distribution solves the equilibrium distribution. [4,8]:

$$E_i(r,u) = r\left(\frac{1-d_0}{b} + \frac{D}{c^2 b} c_i \cdot u + \frac{D(D+2)}{2c^4 b}(c_i \cdot u)^2 - \frac{Du^2}{2c^3 b}\right) \quad (6)$$

Here b is the velocity of sound and D and d_o are constants. A lattice that is isotropic and Galilan invariant can be recovered by setting D=2, b=6, and d_o = ½[4].

3. Computational Implementation of the LBGK Method

The mathematical method was implemented into C code and constructed in such a manner that the Benchmark cases would be easily simulated. The use of a right circular cylinder and setting boundary conditions involved the placement of objects on the lattice.

When a fluid particle encounters an object on the lattice, the fluid particle is simple rebounded off the object in the direction it originated. This is called the bounce-back boundary condition. This can be implemented in the code during the advection phase of the model. An array is created storing the location of the object on the lattice, which is then compared to the fluid location. Should a fluid particle be in the same location as an object the direction of the particle is reverse and moved back to its' previous location.

The bounce-back boundary condition is also used for generation a non-slip boundary condition [8] on the lattice. Placing an object point along one of the boundaries of the lattice does this.

Fluid flow is introduced into the model by redistributing the lattice densities along the first lattice column (left side). This is done by introducing an acceleration constant into the model and decreasing the neighbouring lattice velocities to the left of the first column and increasing lattice velocities to the right of the lattice column. Lattice nodes above and below the selected lattice point are ignored. This causes flow to move across the lattice from left to right.

For the right side of the lattice an outlet boundary condition was imposed. This was done to allow flow to enter at the first lattice column on the left side of the lattice and exit of the right side. This is done by setting the density nodes on the right most lattice column to be 1.0 [1].

There are many different algorithms available for putting this type of model into computational code. The different methods are usually developed out of the need for efficiently and computational speed. The method chosen is not efficient, but is the most straight forward. The following pseudo code shows how this model was implemented.

Start Program
Read in Obstacle Location File
Set initial density distribution
Loop for T time steps
{
Redistribute along first lattice column
Propagate fluid particles
Check for obstacle (bounce-back)
Calculate density and velocity moments through Eq. (5)
Calculate Relaxation through Eq. (6)
}
Write velocity and pressure data to file
End

4. Right Circular Cylinder Benchmark

The first benchmark that will be conducted on the LBGK model is fluid flow past a right circular cylinder. This type of test will determine if the model is capable of handling flow past objects and maintaining physical accuracy. This will be done through a comparison to the analytical solution.

i) The Analytical Solution for velocity

A right circular cylinder with radius a is placed in an initially uniform flow of an incompressible fluid. The flow will tend to a uniform velocity V_o in the x direction at large distances from the cylinder. The cylinder is placed inside a domain with length X and height Y.

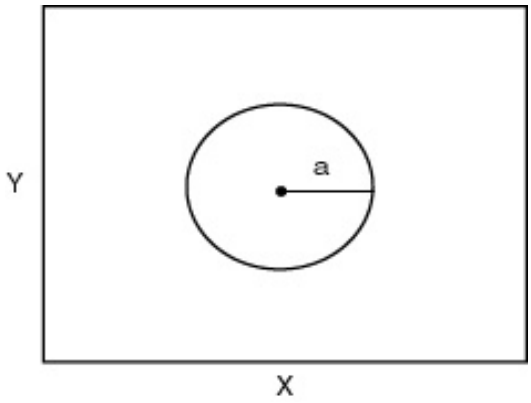

Figure 2: Right circular cylinder with radius a on lattice with dimensions X and Y.

Taking the velocity vector $\vec{V}$ in the xy-plane of flow we can relate the velocity vector to the velocity potential using polar coordinates. [5]

$$\vec{V} = \vec{U_r}\frac{\partial j}{\partial r} + \vec{U_q}\frac{1}{r}\frac{\partial j}{\partial q} \quad (7)$$

The velocity potential will now be constrained to satisfy the continuity equation $\nabla^2 j = 0$. In polar coordinates this becomes:

$$\frac{1}{r}\frac{\partial}{\partial r}\left(r\frac{\partial j}{\partial r}\right) + \frac{1}{r^2}\frac{\partial^2 j}{\partial q^2} = 0 \quad (8)$$

The flow will be prevented from passing through the cylinder and the flow will be constrained to rotate around the cylinder. These conditions are met by applying the following boundary conditions:

$$\frac{\partial j\,(a,0)}{\partial r} = 0 \quad (9) \qquad \frac{\partial j\,(\infty,0)}{\partial r} = V_0\cos(q) \quad (10)$$

Through the imposition of these boundary conditions the solution to (8) is easily found to be: [5]

$$j\,(r,q) = c_o + kq + V_o\left(r + \frac{a^2}{r}\right)\cos q \quad (11)$$

Here c_o and k are arbitrary constants. One can then express the velocity vector (7) in polar coordinates.

$$\vec{V} = \left[V_0\left(1-\frac{a^2}{r^2}\right)\cos(q)\right]\vec{U_r} - \left[V_0\left(1+\frac{a^2}{r^2}\right)\sin(q)\right]\vec{U_q} + \frac{k}{r}\vec{U_q} \quad (12)$$

In order for meaningful comparisons to be made when examining the LBGK model, it is necessary to look at the streamlines of the flow potential. The solution for streamline solutions found from (8) are: [5]

$$j\,(r,q) = d_o - k\log r + V_o\left(r + \frac{a^2}{r}\right)\sin q \quad (13)$$

Here d is another arbitrary constant. A stream function is found by examining points of constant velocity flow along the lattice. The solution to the stream function expressed in Cartesian coordinates is: [5]

$$V_0 y\left(1-\frac{a^2}{x^2+y^2}\right) - \frac{k}{2}\log(x^2+y^2) = const \quad (14)$$

Using equations (12) and (14) some measurable properties of the fluid flow that can be used for comparison will be known. From our applied boundary conditions, the fluid circulation will be centred about the centre of the cylinder. This also means that the fluid will be vortex free.

The velocity potential constant kq gives the rate of circulation about the cylinder. The flow will rotate around the cylinder at the constant rate proportional to k. In other words, the circulation about any distance r from the cylinder should be constant. This also means that at different radii from the centre of the cylinder, the expected velocity magnitude will be related by:

$$|V| = \frac{k}{r} \quad (15)$$

The LBGK model should exhibit all these behaviours to be considered to be accurate.

ii) Benchmarking velocity

Several simulation of the right circular cylinder benchmark was carried out with the LBGK simulation. The lattice size was set at 300x200. The Reynolds number Re=3 was used with a time relaxation parameter $\tau = 0.005$. The acceleration of the fluid was set at 1.25. A right circular cylinder with a radius of 5 node points was placed on the grid. No slip boundary conditions were imposed along the top and bottom of the lattice through the placement of obstacles along the edges of the lattice. A source and sink were placed at the left and right edges of the lattice to induce flow through a body force. The simulation was run for 5000 time steps and the results were extracted at the end of the run.

Figure 3 displays a greyscale image of the simulation output for the x-velocity component of the fluid flow. A qualitative examination of the diagram shows realistic flow behaviour. Flow velocity before and after the cylinder appears to be moving at a constant velocity. The flow impacting the front of the cylinder slows down due to the collision with the cylinder and the fluid particles moving from behind. The flow velocity increases while moving around the cylinder and continues on its path. There is a clear boundary layer along the surface of the cylinder. Also, some rotation is apparent behind the cylinder where the flow curves around to the backside of the sphere. (The x-velocity moves in the negative direction in this region.)

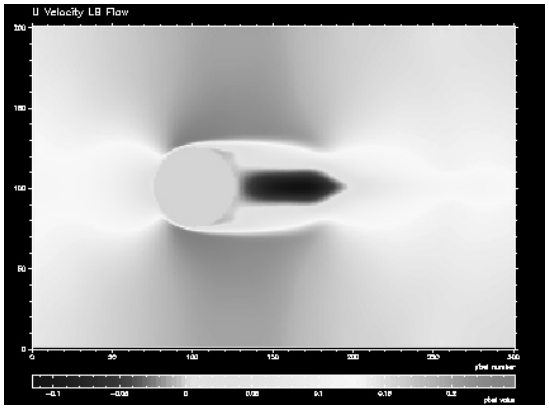

Figure 3: The x-velocity component of flow past a right circular cylinder.

Figure 4 displays the y-velocity component of the fluid flow in this simulation. Again, a qualitative examination of this figure shows the expect behaviour of fluid flow past a right circular cylinder. At the front surface of the cylinder, one can see the fluid moves in a sharp upwards and downwards direction as the fluid moves around the cylinder surface. Behind the cylinder, two components are apparent. Downstream, the flow returns to its' original flow path with another region of upwards and downward flow movement. Directly behind the surface of the cylinder, there are two regions displaying y-component velocity. By comparing this region to the same region in Figure 3 it is quite apparent that there is an onset of rotational motion directly behind the cylinder. This is also expected flow behaviour for this benchmark.

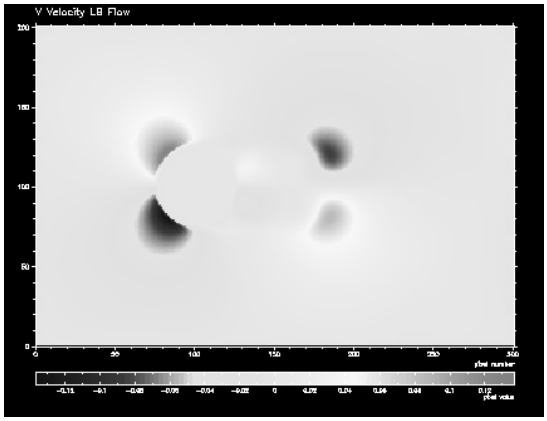

Figure 4: The y-velocity component of fluid flow past a right circular cylinder.

Turning to a quantitative evaluation of the LBGK model performance, the behaviour of fluid velocity magnitude as a function of radii from the centre of the cylinder will be examined through the relationship given in equation (15). Figure 5 below shows model output of the velocity magnitude in a vertical cross section through the centre of the cylinder. By examining the figure it is quite apparent that the expected behaviour is seen in the LBGK model. The velocity magnitude increases from a constant flow rate in the manner given in (15). The velocity then drops sharply in the region of the surface of the cylinder. The velocity magnitude then decreases to the same constant velocity in the same behaviour expected via equation (15).

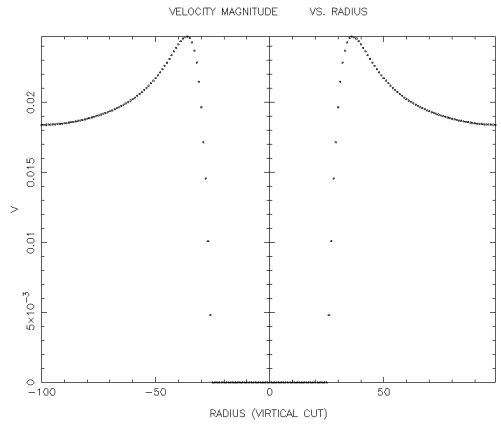

Figure 5: Vertical cross section of lattice displaying velocity magnitude of fluid flow past a right circular cylinder. Compared to Equation (15) the expected results are obtained.

Figure 6 seen below shows a velocity magnitude in a horizontal cross section of the grid through the centre of the cylinder. The behaviour seen here is also what was expected from our knowledge of flow behaviour past circular cylinders.

The flow in front of the cylinder starts to drop dramatically as it approaches the surface. With the cylinder centred on the zero position and a radius of 25 node points, one can see that the velocity magnitude will start to decrease almost immediately upstream from the cylinder's surface. This indicates a build up of fluid density and pressure in the lattice. This build up and upstream influence of the object is a strong indication of a physical flow. Laminar flow at low Reynolds numbers has the property of being effected up stream by the influence of down stream objects. With this behaviour being exhibited, it is apparent that the collision operator in the model is doing a good job. The flow behaviour down stream of the cylinder appears to fluctuate and then stabilize. This is due to the rotational motion and drag force influence of the object. This kind of behaviour is also expected and the model appears to be doing a very good job.

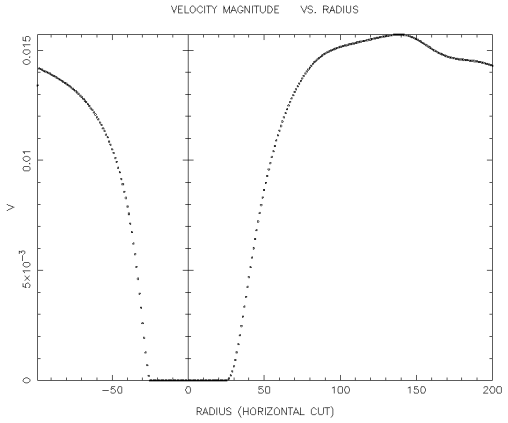

Figure 6: Horizontal cross section of the lattice displaying the velocity magnitude of fluid flow past a right circular cylinder.

Using the data extracted and displayed in Figures 5 a comparison of the data to the analytical solution is made. Figure 7 displays a comparison between the analytical solution (solid line) and the simulation results. One can see that the simulation is in good agreement with the analytical solution away from the surface of the cylinder. Around the surface of the cylinder there is a deviation between the two curves.

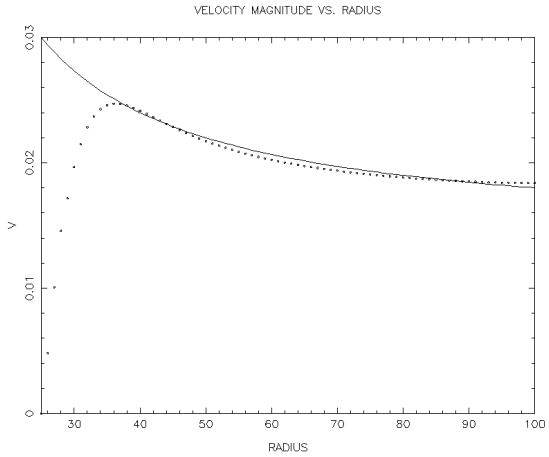

Figure 7: Velocity magnitude vs. distance radius. (dashed line: simulation, solid: analytical)

In Figure, 8 the error profile of Figure 7 is displayed. It is quite apparent from the figure that the behaviour of the velocity that there is an increase in error just before the surface of the cylinder.

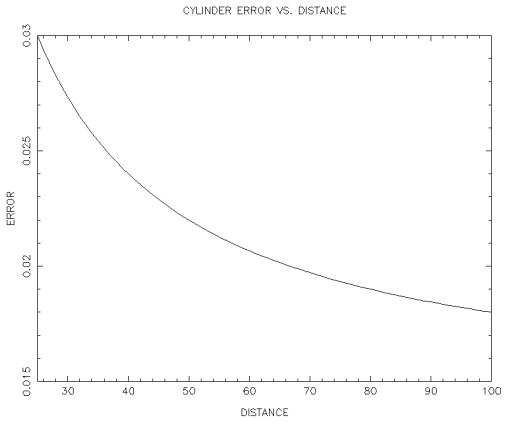

Figure 8: Error of simulation compared to analytical solution. The simulation deviates from the analytical solution around the surface of the cylinder.

The error increase can be accounted to two different properties of the physical behaviour of fluid flow and the LBGK model. When fluid flows around an object, it is expected that a boundary layer will form around the surface of the cylinder and be of a finite thickness. These boundary layers are abrupt changes in the fluid behaviour, which can account for the increase in error. Also, this increase in error is due to the bounce-back boundary conditions when the fluid particles encounter the object. It is expected that the bounce back properties would have influence on the fluid motion for several lattice points away from the surface of the object.

5. Poiseuille Channel Flow Benchmark

i) Analytical Velocity and Pressure Solutions

The LBGK model was then benchmarked by implementing a steady fluid flow in a channel with a width of 2L. No slip boundary conditions are imposed through the introduction of walls at the top and bottom of the lattice. This benchmark provides a way to check the behaviour of the pressure and velocity of the fluid flow.

The analytical solution for the pressure is found by taking into consideration that fluid flow is driven by a constant force of $Q = qV_x$ [8,9]. This leads to an acceleration of the fluid in the channel with a value of gV_x [8]. The expected pressure fields in this situation are outlined in [8] and the effective pressure for a given location in the channel is found by:

$$P_{eff} = c_s{}^2 \Delta r - \overline{r} g x \quad (16)$$

Here c_s is the speed of sound in the fluid, Δr is the local change in density, $\overline{r}$ is the average pressure in the channel, and x is the distance from the channel inlet [8]. The LBGK model should exhibit the same behaviour as the solution given in (16).

In this situation the Poiseuille flow reduces the Navier-Stokes equation to an ordinary differential equation [9].

$$u \frac{d^2 V_x}{dy^2} + Q = 0 \quad (17)$$

Here ν is the viscosity of the fluid. By applying the boundary conditions such that $V_x = 0$ at y=-L and y=L the analytical solution is found [9].

$$V_x(y) = \frac{Q}{2u}\left(L^2 - y^2\right) \quad (18)$$

This is a parabolic solution that gives the velocity profile of the fluid in the channel. The LBGK model should give an x-component fluid velocity that is a maximum at the centre of the channel that decreases in a parabolic fashion towards the walls.

ii) Benchmarking Velocity

Testing for velocity using the Poiseuille Channel benchmark, the model was run in a channel with a length of 50 and width of 25 lattice points under no-slip boundary conditions. The acceleration was set a 0.005 and grid density 0.1. The time relaxation parameter was set at 1.85. The viscosity of the fluid was set at 0.0135 with a Reynolds number of 4.3. The model was

run for 3000 time steps and the data was extracted at the end of the simulation. Figure 9 displays a grey scale diagram of the velocity magnitude of the fluid flow.

Figure 9: Grey scale diagram of the fluids Velocity magnitude in a Poiseuille Channel flow simulation.

Using equation (18) the x-velocity component was compared to the analytical solution. Figure 10 shows the velocity profile of the fluid by taking a vertical cut of the channel at a length 25. . The solid line is the analytical solution, and the points are the data results obtained from the simulation. The analytical solution shows that the velocity flow profile in the channel is parabolic. The flow velocity will be highest at the middle of the channel. The simulation shows to be within excellent agreement with this behaviour.

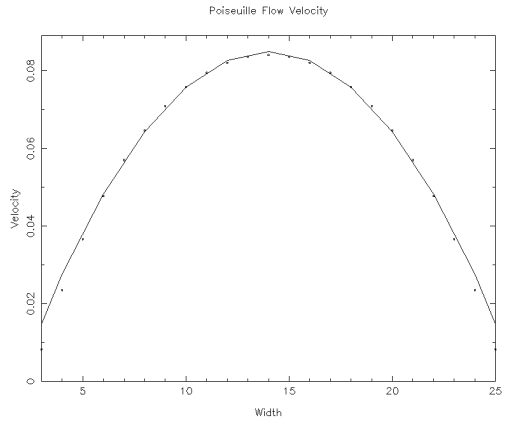

Figure 10: X-Velocity component profile of channel flow at length 50. Solid line is the analytical solution. Points are LBGK simulation results.

Figure 11 shows an error profile of the simulation compare to the analytical solution along the width of the channel. There is excellent agreement between the simulation and the analytical solution in the middle of the channel. It is apparent that there is a slight deviation of the simulation from the analytical solution along the sides of the channel. However, there is a slight deviation of the simulation from the analytical solution along the sides of the channel. The increase in error at the sides of the simulation is extremely small, and in most situations can be ignored. However, if very high accuracy is needed along the boundaries then this increase in error could be a cause for concern.

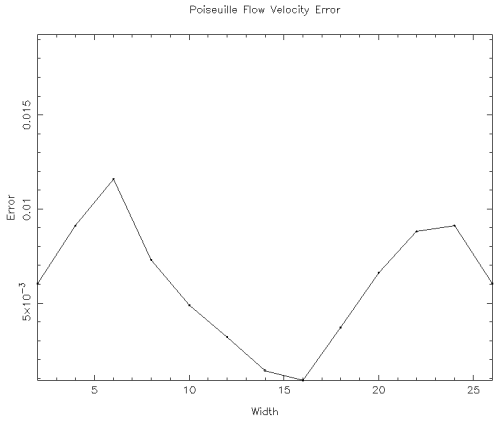

Figure 11: Error profile of channel flow.

iii) Benchmarking Pressure

The analytical solution for the expected pressure profile of Poiseuille channel flow is given by equation (16). Using the same data obtained from the simulation run in section 6.iii a benchmark of the pressure behaviour was made.

If one examines equation (16) it is quite easy to see that the expect pressure should linearly decrease from the inlet from the channel. Figure 12 below displays a grey-scale diagram of the pressure through the channel.

Figure 12: Grey-Scale diagram of Fluid pressure through Channel.

The pressure is the highest at the first lattice column on the left (source) and the lowest at the final lattice column on the right (sink). A qualitative examination of the graph reveals the

drop in pressure along the channel appears to be linear.

A quantitative comparison between the analytical solution and the LBGK results was made. Figure 13 shows the drop in pressure along the length of the channel.

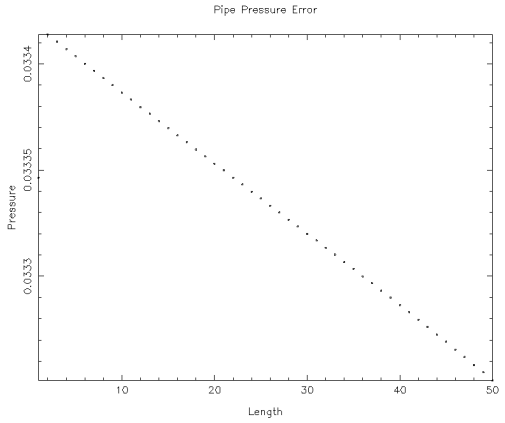

Figure 13: Analytical and LBGK pressure values along channel length. The difference between the analytical solution and simulation almost zero**.**

The difference between the analytical solution and the simulation output is virtually non-existent. The drop in pressure is linear as expected. The LBGK model appears to be doing exceptionally well while handling the pressure distribution in this situation.

6. Times for Simulation Stabilization

One of the difficulties of LBGK models of this type is that it can take time for the model to reach a stable state before the simulation can be considered accurate. When a flow is induced across the lattice, as was done in this simulation, it will take time for the particles to distribute themselves across the lattice. This leads to fluctuations in the behaviour of the flow until the model has time to settle down into a stable state.

Figure 14 shows the average velocity of the model after each time step. Since the fluid is undergoing linear acceleration, a linear increase in the average flow velocity is expected. It is quite apparent from the figure that there are strong fluctuations in the average velocity up to about 700 time steps and small fluctuations in the velocity up to 1500 time steps. Other experiments show that the amount of time required for the LBGK model to settle into a stable state strongly depends on the physical situation being modelled and the size of the lattice.

The computational scientist must take this behaviour of the LBGK model into consideration. If the model is not allowed to settle into a stable state, then the results will not be reliable.

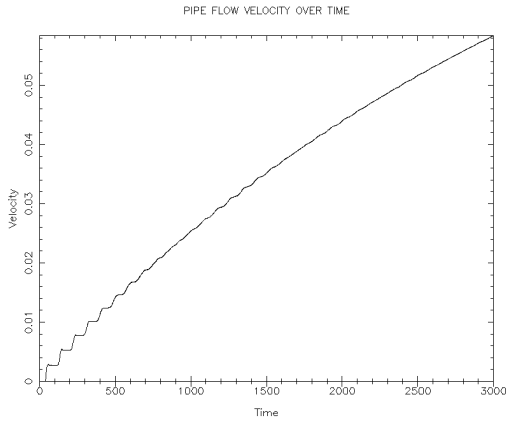

Figure 14: Average velocity over simulation time. Notice velocity fluctuations early in the simulation.

7. Discussion and Conclusion

It is quite clear that the benchmarks tested with the LBGK model have been very successful is revealing the model's capabilaties and limitations. Most importantly, each benchmark provided a way of defining these limitations in a quantitative manner.

The right circular cylinder benchmark showed us that the model was capable of handling fluid flow around objects in a physically accurate manner. The velocity profiles of the fluid flow around the cylinder turned out to be very accurate when compared to the analytical solution. The benchmark also revealed that the bounce-back boundary conditions allowed for the manifestation of a boundary layer along the surface of the cylinder, which is a physically accurate depiction of fluid flow.

The Poiseuille channel flow benchmark revealed more insight into the behaviour of the model. The velocity profile of a cross section in

the channel revealed that the LBGK results were excellent when compared to the analytical solution. In this test it was also found that velocity error was slightly higher at the edges of the channel. The error in this situation was very tiny, but it could be a cause of concern in certain situations.

The Poiseuille channel flow benchmark also provided great insight into the behaviour of the pressure in the model. The pressure fields obtained were beyond expectations and matched the analytical solutions almost exactly.

There are still several factors that should be examined in this model to have a complete understanding of the constraints and limitations of the LBGK model. The behaviour of pressure fields in the presence of objects should be examined. Also, due to the fact that the LBGK model is restricted to low Reynolds numbers, the upper limits of flow velocity should be found.

The cause of the slight error at the sides of the channel in the Poiseuille benchmark should be found. It is quite possible that this error introduced is caused by the bounce-back boundary conditions or because of shear stress.

Though there is still more testing to be done on this model, through the use of the benchmarks, it is apparent that the model can be trusted to produce good results in similar situations.

8. References

[1] A. M. Artoli, A. G. Hoekstra, P. M. A. Sloot, Accuracy of 2D Pulsatile Flow in the Lattice Boltzmann BGK Model. *Lecture Notes in Computational Science*, **2329** ISBN 3-540-43591-3, 2002.

[2] Bruce Boghosian, Lattice gases and cellular automata. *Future Generation Computer Systems*, **16**: 171-185, 1999.

[3] Meng Wang, Pietro Catalano, Prediction of high Reynolds number flow over circular cylinder using LES with wall modelling. *Centre for Turbulence Research Annual Research Briefs 2001*.

[4] James Buik, *Single Relaxation Time Lattice Boltzmann Model*. University of Edinburg web pages.

[5] Francis B. Hildebrand. *Advanced Calculus for Applications*. Prentice-Hall, Inc., Englewood Cliffs, New Jersey, 1963.

[6] D.G. Zill, M.R. Cullen. *Differential Equations with Boundary Value Problems*. Brooks/Cole, Pacific Grove, California 1986.

[7] M. Bouzidi, D. d'Humieres, P. Lallemand, L. Lou. Lattice Boltzmann Equation on a Two-Dimensional Rectangular Grid. *Journal of Computational Physics*, **172** 704-717, 2001.

[8] D. Kandihai, A. Koponen, A. Hoekstra, M. Kataja, J. Timonen, P. M. A. Sloot. Implementation Aspects of 3D Lattice-BGK Boundaries, Accuracy, and a New Fast Relaxation Method. *Journal of Computational Physics*, **150** 482-501, 1999.